Villa C., Gaudio D., Cattaneo C., Buckberry J.,Wilson AS., Lynnerup N. 2015. *Surface curvature of pelvic joints from three laser scanners: separating anatomy from measurement error.* Journal of Forensic Sciences Vol. 60, No. 2, 2015, p. 374–381.

Surface curvature of pelvic joints from three laser scanners: separating anatomy from measurement error.

Chiara Villa[1], M.Sc., Daniel Gaudio[2], Ph.D., Cristina Cattaneo[2], M.D., Ph.D., Jo Buckberry[3], Ph.D., Andrew S.Wilson[3], Ph.D. and Niels Lynnerup[1], M.D., Ph.D., D.M.Sc.

[1]Laboratory of Biological Anthropology, Department of Forensic Medicine, University of Copenhagen, Denmark;

[2]LABANOF, Forensic Anthropology and Odontology Laboratory, Department of Human Morphology, University of Milan, Italy.

[3]Biological Anthropology Research Centre, Archaeological Sciences, University of Bradford, UK;

Corresponding author:

Chiara Villa

Laboratory of Biological Anthropology,

Department of Forensic Medicine,

University of Copenhagen,

Frederik V's Vej 11, DK-2100 Copenhagen, Denmark.

Email: chiara.villa@sund.ku.dk

Villa C., Gaudio D., Cattaneo C., Buckberry J.,Wilson AS., Lynnerup N. 2015. *Surface curvature of pelvic joints from three laser scanners: separating anatomy from measurement error*. Journal of Forensic Sciences Vol. 60, No. 2, 2015, p. 374–381.

Abstract

Recent studies have reported that quantifying symphyseal and auricular surfaces curvature changes on 3D models acquired by laser scanners have a potential for age estimation. However, no tests have been carried out to evaluate the repeatability of the results between different laser scanners. 3D models of the two pelvic joints were generated using three laser scanners (Custom, Faro, Minolta). The surface curvature, the surface area and the distance between co-registered meshes were investigated. Close results were found for surface areas (differences between 0.3% and 2.4%) and for distance deviations (average < 20 μm, SD < 200 μm). The curvature values were found to be systematically biased between different laser scanners, but still showing similar trends with increasing phases / scores. Applying a smoothing factor to the 3D models, it was possible to separate anatomy from the measurement error of each instrument, so that similar curvature values could be obtained ($p < 0.05$) independent of the specific laser scanner.

Keywords: forensic science, forensic anthropology, pubic symphysis, auricular surface, curvature, laser scanner, surface area, distance deviation, 3D models

Recent studies have shown the benefits of quantitative methods using 3D laser scanner models in addressing fundamental issues in physical and forensic anthropology. Sexual dimorphism and population and ancestry variation have been investigated quantifying surface areas or extracting curves (1-5). The morphological features of the symphyseal and the auricular surfaces used for age estimation have been examined looking at the surface curvature changes (6-8). Laser scanners have also been used to investigate cranial facial variation and for facial identification (9-13).

In all these applications, the precision and the repeatability of the measurements among different instruments are essential for the reliability of each method; in fact, there are different models of laser scanners and differences between the software used for post-processing the scans (i.e. aligning, merging and fusion of the single scans to create a 3D model). It has been demonstrated that the surface areas were reproduced with high precision and the measurement errors of the extracted information varied from 0.2% to about 1% (5, 14); it has been also shown that the location of points on the surface (landmarks) and the measurements of length could be accurately repeated on 3D models (11, 12, 15). When some of the parameters used for the scans made by the same laser scanner have been changed, measurement error was reported to increase slightly to 2% (14). However, all these studies have tested the repeatability of measurements made by the same instrument.

Laser surface scanning (and CT-scanning) of bones is proposed as a method to make osteological data more widely and easily available, e.g. the Smithsonian 3D collection (16), "Digitised Diseases" (17) and "From Cemetery to Clinic" (18). It is thus important to investigate whether 3D models acquired by different laser scanners may exhibit larger differences than those acquired by the same scanner. Irrespective of the performance of each laser scanner, the nodes of the resulting 3D model surfaces represent the true anatomical shape, plus some error due to measurement uncertainty. The formal expression of this uncertainty is difficult, as it requires full knowledge not only of the

instrument and object properties, but also of operational details which may not always be available, such as calibration steps followed and the exact distance between object and scanner (19, 20). A simple but general approach to assess measurement error that does not rely on any external knowledge beyond the scanned 3D mesh would therefore be particularly convenient. We assumed the measurement uncertainty manifests itself exclusively as independent random error in the position of mesh nodes, which can be effectively reduced by a smoothing operation over neighboring nodes. If this assumption is appropriate, the use of an adequate amount of smoothing would filter out the measurement error while preserving the overall anatomical shape of the bone surface, and homogenize 3D models from different instruments. The aim of this paper was to experimentally verify the validity of our assumption by using 3D models of symphyseal and auricular surfaces generated with three different laser scanners, three different kinds of post-processing software, and the same algorithm used in Villa et al. (6). To approximate the conditions of an independent replication of this experiment, only the final 3D models were compared, excluding other influences such as the resolution of the instrument, the operational conditions or type of algorithm used to merge the scans.

Materials and methods

Sample

The sample consisted of the 24 Suchey-Brooks pubic bone casts (12 females, 12 males) (21) and 19 archeological auricular surfaces of the "recording kit" collected by Buckberry and Chamberlain as illustrative of the different scores of the features described in their method (22). We selected only the central area of the pubic symphyseal face inside the margins and the internal area of the auricular surface, i.e. the area delimitated by the contour of the joint, as described in (6).

Laser scanning

Three different laser scanners were used in this study (Table 1): FaroArm Quantum with V3 Laser Line Probe - FARO Singapore Pte. Ltd (abbreviated Faro), property of the University of Bradford (UK); Minolta VI-910 - Konica Minolta Sensing, Inc. Osaka-Japan (abbreviated Minolta), property of the University of Milan (Italy); and a custom laser scanner (abbreviated Custom) property of the University of Copenhagen (Denmark) (6). The Faro is equipped with an articulated arm, thus the object to scan was kept fixed during the scanning process; for the other two laser scanners, the scanning system was fixed while the object was moved. In order to capture as much detail as possible, the object was located as close as the laser scanner allowed.

Three different software applications were used for the post-processing: PolyWorks (23) was the software accompanying the Faro instrument, Geomagic Studio (24) was used for the scans from Minolta and David-laser scanner software (25) for those from Custom. In each software, the followed steps were carried out: first, each mesh was visually inspected, and occasional spikes were removed and small holes were filled; second, the individual meshes were aligned (the Faro roughly aligned the individual scans during the scan processing, so a second alignment was performed in this case); third, the aligned meshes were merged for generating the final mesh and removing redundant data; finally, a slight smoothing (the lowest possible smooth allowed by each software) was applied at the merged mesh. The final model was saved in STL format (Standard Triangulation Language) and used in all analysis.

Many factors can have an effect on the scans and are difficult to control and reproduce. First, the performance of the different laser scanners rarely can be compared since there are no protocols and the precision and accuracy specified by different manufacturers are measured and expressed in different ways (26). Furthermore, the quality of the resulting 3D models depends not only on the nominal resolution of the laser scanner, but also, among other factors, on the ambient light, the manual

skill of the operator (more evident in Faro), surface color and the geometry of the object, the distance of the scanner to the object and the instantaneous incident angle of the laser and the line of sight of the camera (19, 20). We were only interested on the differences among the final 3D, so the scans were acquired under optimal conditions by qualified operators. While this may not be the most formally rigorous experimental protocol, it can be argued that it provides the most relevant common ground for comparison among instruments under operational circumstances as close as possible to the real world application of these instruments. As we are only concerned with the practical usability of the typical scans a user will obtain, we have focused on comparing the final 3D models, without emphasizing these other factors further.

Surface curvature

Curvature can be defined as the variation of a geometrical object (i.e. a curve or a surface) from being flat. Mathematically, the curvature (K) in two-dimensional space can be defined as the reciprocal of radius (R) of an osculating circle (K = 1/ R), where the osculating circle is the circle that most closely approximates the curve at a given point. In three dimensions, the curvature depends on the principal curvatures of two orthogonal planes. These describe the maximum curvature (K_{max}) and the minimum curvature (K_{min}) and these two curvatures can be combined in several ways. The *extrinsic curvature* or *mean curvature* (K_m) is used in this study and is defined as the average of the two curvatures, espressed as $K_m = (K_{max+}K_{min})/2$. Conventionally, convex surfaces will yield positive values and concave surfaces negative values, respectively (see (27), for further mathematical explanation). The extrinsic curvature has been calculated using Peyre's Toolbox Graph MATLAB software (28), adapting some of the scripts (29). For each specimen scanned by each laser scanner, we calculated the arithmetic mean of the absolute values of curvature used in Villa et al. (6). Therefore, we calculated the curvature of 57

three-dimensional models of auricular surfaces (19 specimens scanned three times) and 72 three-dimensional models of pubic bones, (24 casts scanned three times). The differences between the 3D models of the same specimen were calculated and expressed in percent. The curvature values of 3D models from Custom laser scanner were used as reference models, since they were used in previous work (Villa et al. (6)). To eliminate the measurement error of each laser, a different smoothing factor was used to reduce the total curvature differences to a maximum of 2%. The smoothing factor controls the progressive denoising of the signal, based on the immediately adjacent surrounding points (28). This procedure did not alter the surface features, which are at a much larger scale, but only eliminate the point-to-point measurement error of each laser scanner. No alteration of surface osteological features could be visually observed.

Surface areas and distances

To enable a comparison with other studies reported in the literature, we quantified the surface areas (reported in cm^2) and the differences of surface area (expressed in cm^2 and percent) among the 3D models of the different instruments. In additional, we calculated the distance deviation (reported in μm), i.e. the distance between the points of a 3D model of one laser and corresponding ones of second laser scanner. We used a function of Geomagic Studio Software, called "deviation", that returned for each two-by-two comparison the "Average distance and the "Standard Deviation distance"; furthermore this function generated color-coded mapping of the differences, highlighting the areas and the specimens with problems.

Statistical analyses

All descriptive statistics (means, standard deviations (SD), and differences) were calculated using SPSS software, version 20. We used scatter plots to undertake a visual evaluation of the distances between 3D models from different laser scanners. Each scatter plot shows the comparison between two laser scanners: 1) Faro versus Minolta; 2) Custom versus Faro; 3) Custom versus Minolta. To highlight any variation with increasing age, we ordered the auricular surface features based on increasing score; the features were used in the following order: TO= transverse organization, ST= surface texture, MA= macroporosity, MI= microporosity, AC= apical change. In the same way, we ordered the pubic bones based on increasing phase; two values were present for each phase, representing the early (E) and the advanced (A) patters. The scatter plots were also used to investigate the curvature values, with the same organization described above; in this case, each series represented a laser scanner: Faro, Minolta and Custom. Finally, we performed Kruskal-Wallis ANOVA to compare the revised curvature values, after the use of the smoothing.

Results

Surface curvature

The curvature values of the auricular surface and the pubic bone (male and females separately) are shown in Figure 1. The scatter plots in the column "a" (on the left) show the results obtained using the unmodified algorithm used in Villa et al. (6), with the same smoothing factor for all laser scanners. The curvature values show similar trends with increasing phases and scores: the curvature increases and decreases in the same manner in all three laser scanners, but with a systematic difference among the models of laser scanners. Faro shows the highest curvature values in all samples, both for the pubic bones and the auricular surfaces. Minolta and Custom have closer values, but more than 50% of the curvature values of Minolta are higher than those from Custom, especially in the auricular surfaces. In the pubic bones, differences of 28.8% (females) and 20.5% (males) were found between Faro and Custom, 0.29% (females) and 1.6% (males) between Custom and Minolta. Differences of 44.2% and 9.7% were found in the auricular surfaces, between Faro and Custom, and between Minolta and Custom respectively. To reduce these curvature differences, we modified the amount of smoothing in the curvature algorithm. The curvatures of Faro could be homogenized with Custom using a smoothing factor of 10 for the male pubic bones, of 15 for the female pubic bones, and 20 for the auricular surfaces (Fig. 1, column “b”); in this manner, the distance between the two lasers were reduced to about 1.5%. The curvature values of Minolta and Custom in the pubic bones for both sexes were already very close, with a difference lower than 2%, so no further smoothing factor was applied. A smoothing factor of 5 was required to reduce the difference between the auricular surfaces of Minolta and Custom to 1.8%. Figure 1b (scatter plots on the right) show the corrected curvature values. We found no statistically significant difference ($p > 0.05$) between the corrected curvatures values produced by the different laser scanners.

Surface areas

The measurements of the surface area and differences between the laser scanners for the auricular surfaces and the symphyseal surface (males and females separately) are reported in Table 2. The largest difference for the auricular surfaces was 0.15 cm^2 and was found between Faro and Minolta corresponding to 1.5%. In the symphyseal surface, Custom and Faro have the highest differences, -0.08 cm^2 (2.4 %) in females and -0.05 cm^2 (1.9%) in males.

Distance deviations

Figure 2 show the distributions of the "average distances" (black solid points) and average plus/ minus the SD for the auricular surfaces. It is clear that there is more variation in distances (most evident in the SD) in the last scores where the surface topography is more irregular: score 3 for AC, scores 4 and 5 for TO and ST. This is more evident in the comparison between Custom and the other two laser scanners. Faro and Minolta show the lowest “SD distance”, less than 100 μm with a mean “average distance” of 1.1 μm (Table 3). The “average distances” are small in all comparisons, ranging from 0.7 to 3.7 μm. For the pubic bones, the “average distances” are similar between laser scanners, varying less than 10 μm (Table 2), while the standard deviations increase and reach values over 100 μm; in particular, in females for the phase I (early and advanced patterns, indicated with E and A in the Figure 3) the “average distances” are different from zero and the “SD distance” are over 200 μm. The more complicated the surface topography is (i.e. having high ridges and deep furrows, showing deep depression or porosity), the more the distance deviations increase. An example can be seen in Figure 4, where the color-coded mapping of the distance deviations between laser scanners are visible for the phase VI advanced pattern of the females: Faro and Minolta show the least difference, indeed the

surface is dominated by green color indicating distance between -0.05 to 0.05 μm; the largest deviation in all three comparisons is in the big depression in the lower part of the pubic symphysis. This is an example of a scan artefact in which the camera of the laser scanner failed to record the laser beam because the depth of the feature and the overhanging edges obscured some of the base of the feature. Other examples, in males phase II advanced and phase IV early, have obscured areas that are very difficult to scan and result in large difference between laser scanners, most noticeable between the Custom and the other two instruments (Fig 3).

Discussion

We used 3D models of symphyseal and auricular surfaces generated with three different laser scanner systems to verify the repeatability of surface curvature analysis among instruments using the algorithm described in Villa et al. (6). Comparing the final 3D models, we found that the overall anatomical shape of the bone surface could be represented independently from the laser scanners: we obtained very low distance deviation between 3D models and differences less than 2.5% in the surface area. The differences between the curvature values, as hypothesized in the introduction, depended on the measurement uncertainty produced by each instrument, i.e. each laser scanner introduces a specific amount of random error in the position of the points. The curvature values showed similar trends with increasing phase or score, although they were found to be systematically biased between different laser scanners. The measurement uncertainty of each instrument could be reduced and the curvature results among laser scanners could be homogenized applying an amount of smoothing directly proportional to the differences between curvature values. We used the highest smoothing in 3D models from Faro that showed the highest differences in curvature values both in the symphyseal and auricular surfaces with

respect to the other two laser scanners. These large differences might be explained by considering the organization of the mesh points: the 3D models from Faro had an unstructured grid, i.e. the points of the mesh were not distributed regularly at the same distance, but they were more concentrated and dense in the areas with more details and more distant and less numerous in the flat areas. In contrast, Custom and Minolta showed similar curvature results probably because both instruments produced 3D models with structured grid. In addition, we noticed that those cases showing the larger distance deviations (for example phase I of the symphyseal surface) still kept the larger differences in curvature values, even after the smoothing. This confirms that the smoothing operation could reduce only the independent random error, not the imprecision in the scans.

Furthermore, our tests strongly confirmed that the surface area can calculate with little error using three different laser scanners. Indeed, we obtained comparable errors to those reported by Sholts et al. (14) and Garvin and Ruff (5). Faro and Minolta showed the smallest difference (less than 1%) in the symphyseal surfaces, while the largest one in the auricular surfaces (1.5%). The larger differences in the symphyseal surface were between Custom and the other two laser scanners, and it could be due to the optical surface properties of the specimens and ambient light, since the Suchey-Brooks pubic bone casts are white and shiny. This may have introduced more noise and imprecision in the scans (19, 20). No correspondence between the results of distance deviations and the difference in surface area were found: in the auricular surfaces Custom and Minolta showed the lowest distances, while in the symphyseal surfaces Custom and Faro were better in the females, Faro and Minolta in the males.

Further analysis needs to identify other factors that can reduce measurement error: process of decimation (i.e. reduction of the number of points in a mesh), or function to transform unstructured grid in structured one, and vice versa, could have a similar effect. We would underline that our results could not be generalized: applying the algorithm described in (6), we detected the features useful for age

estimation in a similar way across different laser scanners. Depending on the nature of the investigation, a high resolution laser scanner can have an impact and perform better. Similarly it is also worth considering other scan technologies such as white light, otherwise known as structured light scanners. Finally, a 3D model can be appropriate for one purpose and not for another; thus the analysis needs to be tested for each specific case (30), since no standard procedures are yet defined. This is a necessary step forward towards enabling practical quantitative surface morphology analysis of 3D bone models.

Conclusions

The overall anatomical shape of the bone surface was reproduced in comparable ways using three different laser scanners, as demonstrated by the close surface areas and the low distance variation between co-registered meshes. However, each laser scanner introduces a specific amount of random error in the position of each measured point that can introduce bias to the results of curvature quantification. By applying an adequate amount of smoothing, it was possible to separate the anatomy signal from the instrumental measurement error, thus making the results of the technique developed in Villa et al. (6) independent of the specific laser scanner.

Villa C., Gaudio D., Cattaneo C., Buckberry J.,Wilson AS., Lynnerup N. 2015. *Surface curvature of pelvic joints from three laser scanners: separating anatomy from measurement error*. Journal of Forensic Sciences Vol. 60, No. 2, 2015, p. 374–381.

Acknowledgements

The authors would like to acknowledge the support of members of the Digitised Diseases team – specifically Emma L. Brown, Tom Sparrow and Andrew Holland who provided support and technical advice.

References

1. Sholts SB, Walker PL, Kuzminsky SC, Miller KW, Warmlander SK. Identification of group affinity from cross-sectional contours of the human midfacial skeleton using digital morphometrics and 3D laser scanning technology. J Forensic Sci. 2011;56(2):333-8.
2. Sholts SB, Warmlander SK. Zygomaticomaxillary suture shape analyzed with digital morphometrics: reassessing patterns of variation in American Indian and European populations. Forensic Sci Int. 2012;217(1-3):234 e1-6.
3. Shearer BM, Sholts SB, Garvin HM, Warmlander SK. Sexual dimorphism in human browridge volume measured from 3D models of dry crania: a new digital morphometrics approach. Forensic Sci Int. 2012;222(1-3):400 e1-5.
4. Ruiz Mediavilla E, Perea Perez B, Labajo Gonzalez E, Sanchez Sanchez JA, Santiago Saez A, Dorado Fernandez E. Determining sex by bone volume from 3D images: discriminating analysis of the tali and radii in a contemporary Spanish reference collection. Int J Legal Med. 2012;126(4):623-31.
5. Garvin HM, Ruff CB. Sexual dimorphism in skeletal browridge and chin morphologies determined using a new quantitative method. Am J Phys Anthropol. 2012;147(4):661-70.
6. Villa C, Buckberry J, Cattaneo C, Frohlich B, Lynnerup N. Quantitative analysis of the morphological changes of the pubic symphyseal face and the auricular surface and implications for age at death estimation. Journal of Forensic Sciences. 2015.
7. Tocheri MW, Razdan A, Dupras TL, Bae M, Liu D. Three Dimensional Quantitative Analyses of Human Pubic Symphyseal Morphology: Can Current Limitations of Skeletal Aging Methods Be Resolved. Am J Phys Anthropol (Suppl34). 2002;155.
8. Biwasaka H, Sato K, Aoki Y, Kato H, Maeno Y, Tanijiri T, et al. Three dimensional surface analyses of pubic symphyseal faces of contemporary Japanese reconstructed with 3D digitized scanner. Leg Med (Tokyo). 2013.
9. Cattaneo C, Cantatore A, Ciaffi R, Gibelli D, Cigada A, De Angelis D, et al. Personal identification by the comparison of facial profiles: testing the reliability of a high-resolution 3D-2D comparison model. J Forensic Sci. [Comparative Study]. 2012;57(1):182-7.
10. Lynnerup N, Clausen ML, Kristoffersen AM, Steglich-Arnholm H. Facial recognition and laser surface scan: a pilot study. Forensic Sci Med Pathol. 2009;5(3):167-73.
11. Park H-K, Chung J-W, Kho H-S. Use of hand-held laser scanning in the assessment of craniometry. Forensic Science International. 2006;160(2–3):200-6.
12. Toma AM, Zhurov A, Playle R, Ong E, Richmond S. Reproducibility of facial soft tissue landmarks on 3D laser-scanned facial images. Orthodontics & Craniofacial Research. 2009;12(1):33-42.

13. Shahrom AW, Vanezis P, Chapman RC, Gonzales A, Blenkinsop C, Rossi ML. Techniques in facial identification: computer-aided facial reconstruction using a laser scanner and video superimposition. Int J Legal Med. 1996;108(4):194-200.
14. Sholts SB, Warmlander SK, Flores LM, Miller KW, Walker PL. Variation in the measurement of cranial volume and surface area using 3D laser scanning technology. J Forensic Sci. 2010;55(4):871-6.
15. Sholts SB, Flores L, Walker PL, Warmlander SKTS. Comparison of Coordinate Measurement Precision of Different Landmark Types on Human Crania Using a 3D Laser Scanner and a 3D Digitiser: Implications for Applications of Digital Morphometrics. International Journal of Osteoarchaeology. 2011;21(5):535-43.
[16] humanorigins.si.edu/evidence/3d-collection.
[17] http://barc.sls.brad.ac.uk/digitiseddiseases/index.php.
18. http://www.barc.brad.ac.uk/FromCemeterytoClinic/
19. Vukasinovic N, Bracun D, Mozina J, Duhovnik J. The influence of incident angle, object colour and distance on CNC laser scanning. International Journal of Advanced Manufacturing Technology. 2010;50(1-4):265-74.
20. Zaimovic-Uzunovic N, Lemes S. Influence of surface parameters on laser 3D scanning. 10th International Symposium on Measurement and Quality Control (ISMQC 2010)September 5-9, Osaka-Japan, . 2010:D4-026-01/04.
21. Suchey JM, Brooks ST, Katz D. Instructions for use of the Suchey-Brooks system for age determination of the female os pubis. Instructional materials accompanying female pubic symphysial models of the Suchey-Brooks system. Fort Collins, Colorado: France Casting. 1988.
22. Buckberry JL, Chamberlain AT. Age estimation from the auricular surface of the ilium: A revised method. Am J Phys Anthropol. 2002;119(3):231-9.
23. http://www.innovmetric.com/polyworks/3D-scanners/home.aspx?lang=en
24. http://www.geomagic.com/en/products/studio/overview/
25. http://www.david-3d.com/?section=Downloads
26. Guidi G, Russo M, Magrassi G, Bordegoni M. Performance Evaluation of Triangulation Based Range Sensors. Sensors. 2010;10(8):7192-215.
27. Da Fontoura Costa L, Jr MCR. Shape Analysis and Classification: Theory and Practice. Boca Raton, Florida: CRC Press LLC, 2000.
28. Peyre G. The Numerical Tours of Signal Processing - Advanced Computational Signal and Image Processing. IEEE Comput Sci Eng. 2011;13(4):94-7.
29. http://www.mathworks.com/matlabcentral/fileexchange/5355 last accessed 20.01.2014
30. Friess M. Scratching the surface? The use of surface scanning in physical and paleoanthropology. Journal of Anthropological Sciences. 2012;90:7-31.

Additional Information and Reprint Requests Section

Chiara Villa, M.Sc.

University of Copenhagen,

Department of Forensic Medicine

Villa C., Gaudio D., Cattaneo C., Buckberry J.,Wilson AS., Lynnerup N. 2015. *Surface curvature of pelvic joints from three laser scanners: separating anatomy from measurement error*. Journal of Forensic Sciences Vol. 60, No. 2, 2015, p. 374–381.

Frederik V's Vej 11

DK-2100 Copenhagen

Email: chiara.villa@sund.ku.dk

Villa C., Gaudio D., Cattaneo C., Buckberry J.,Wilson AS., Lynnerup N. 2015. *Surface curvature of pelvic joints from three laser scanners: separating anatomy from measurement error.* Journal of Forensic Sciences Vol. 60, No. 2, 2015, p. 374–381.

Table 1: Performance parameters of the laser scanners. The accuracy values are taken from the available manufacturers literature. They are not always comparable across instruments and with the actual measurement conditions used in this work (* to scan a pubic bone, (a) volumetric maximum deviation at 1.8m, (b) to the Z reference plane -Conditions: TELE/FINE mode, Konica Minolta's standard, (c) calculated as 0.5% of the object size)

	Portability	**Weight**	**Texture**	**Velocity of scan (*)**	**Type of laser scanner system**	**Accuracy**	**Type of mesh**	**Range of price (€)**
FARO	Yes	~10 kg	No	Fast (less than 5min)	Mobile (object fixes)	0.023 mm (a)	Triangle, unstructured	>50 000
MINOLTA	Yes	~11 kg	Yes, color	Fast (less than 5min)	Fixed (object moves)	[b]X: ±0.22mm Y: ±0.16mm Z: ±0.10mm (b)	Triangle, structured	>50 000
CUSTOM	Yes	~5 kg	Yes, grey scale	Very slow (~15 min)	Fixed (object moves)	0.025- 0.04 mm (c)	Triangle, structured	<5 000

Table 2: Mean value and standard deviation of the surface area of the auricular surfaces and the pubic bones for each laser scanner and area differences in cm and percent

		Surface area (cm^2)			**Area difference (cm^2)**					
	N	**Custom**	**Faro**	**Minolta**	**Custom-Faro**	**%**	**Custom-Minolta**	**%**	**Faro-Minolta**	**%**
Auricular surfaces	19	10.05±4.3	10.09±4.3	9.94±4.1	0.03	0.3%	0.12	1.2%	0.15	1.5%
Pubic bones - Females	12	2.39±0.5	2.44±0.6	2.42±0.5	0.05	1.9%	0.03	1.1%	0.02	0.8%
Pubic bones – Males	12	3.13±0.7	3.21±0.7	3.20±0.7	0.08	2.4%	0.07	2.1%	0.01	0.3%

Villa C., Gaudio D., Cattaneo C., Buckberry J.,Wilson AS., Lynnerup N. 2015. *Surface curvature of pelvic joints from three laser scanners: separating anatomy from measurement error*. Journal of Forensic Sciences Vol. 60, No. 2, 2015, p. 374–381.

Table 3: Deviation distances: average distances and standard deviations (SD) of the auricular surfaces and the pubic bones for coupled laser scanners (all measurements in micrometers - μm)

	Custom vs Minolta		**Custom vs Faro**		**Faro vs Minolta**	
	Average distance	SD distance	Average distance	SD distance	Average distance	SD distance
Auricular surfaces	0.7±2.2	66±38	3.7±4	67±36	1.1±3.6	46±17
Pubic bones – Females	-2.3±14	109±81	-0.7±2.3	70±29	3.9±13.5	77±78
Pubic bones – Males	-4.4±12.2	81±51	2.6±11.9	79±43	0.4±3.1	36±15

Figure 1: Curvature values of the auricular surfaces (top row) and of the pubic bones (middle row females, bottom row males). Column **a** shows the curvatures value with the same "smoothing factor" for 3D models by all laser scanners; Column **b** shows the curvature values with different "smoothing factor" (reported in the legends)

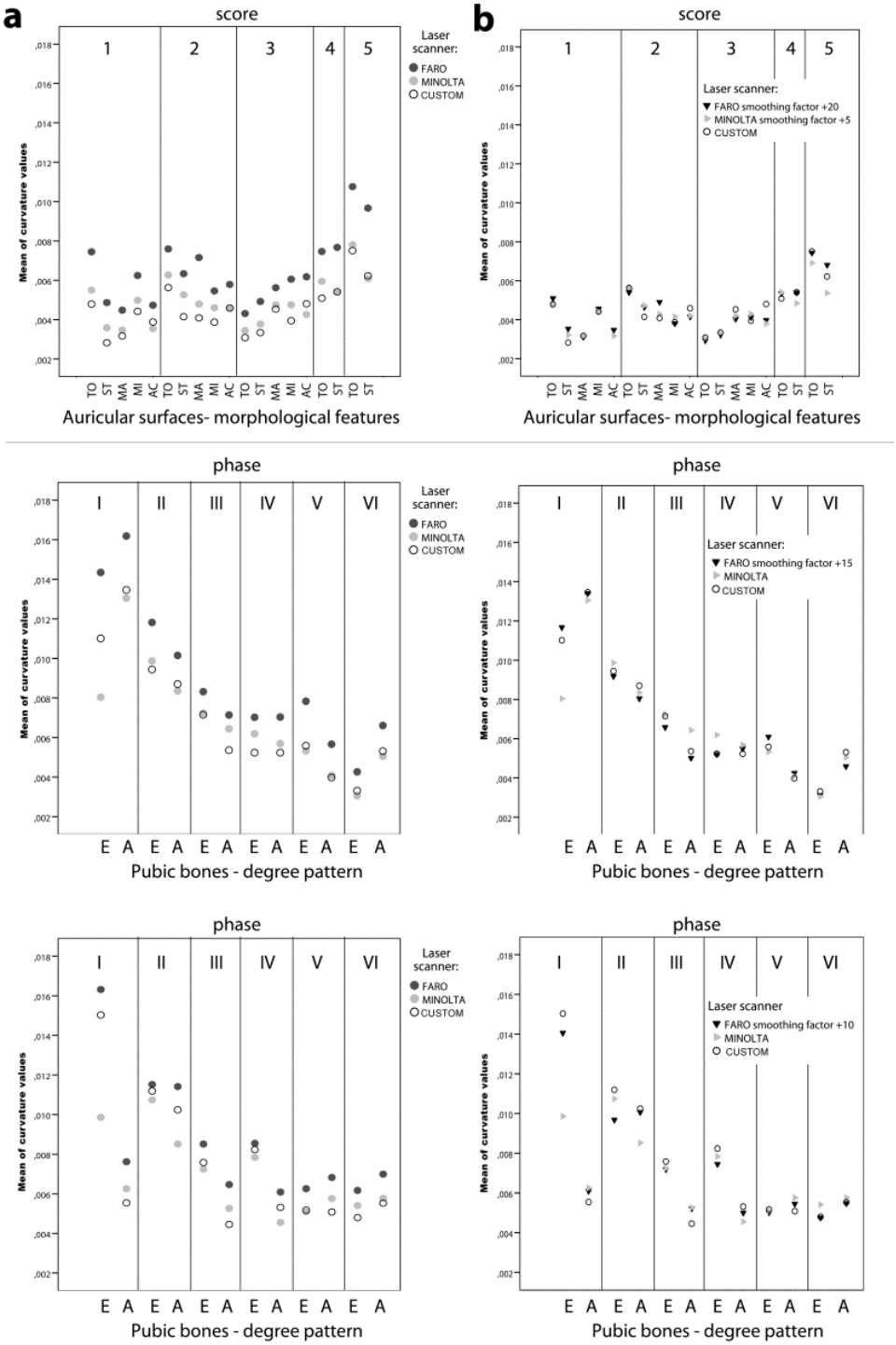

Villa C., Gaudio D., Cattaneo C., Buckberry J.,Wilson AS., Lynnerup N. 2015. *Surface curvature of pelvic joints from three laser scanners: separating anatomy from measurement error*. Journal of Forensic Sciences Vol. 60, No. 2, 2015, p. 374–381.

Figure 2: Auricular surface distance deviation

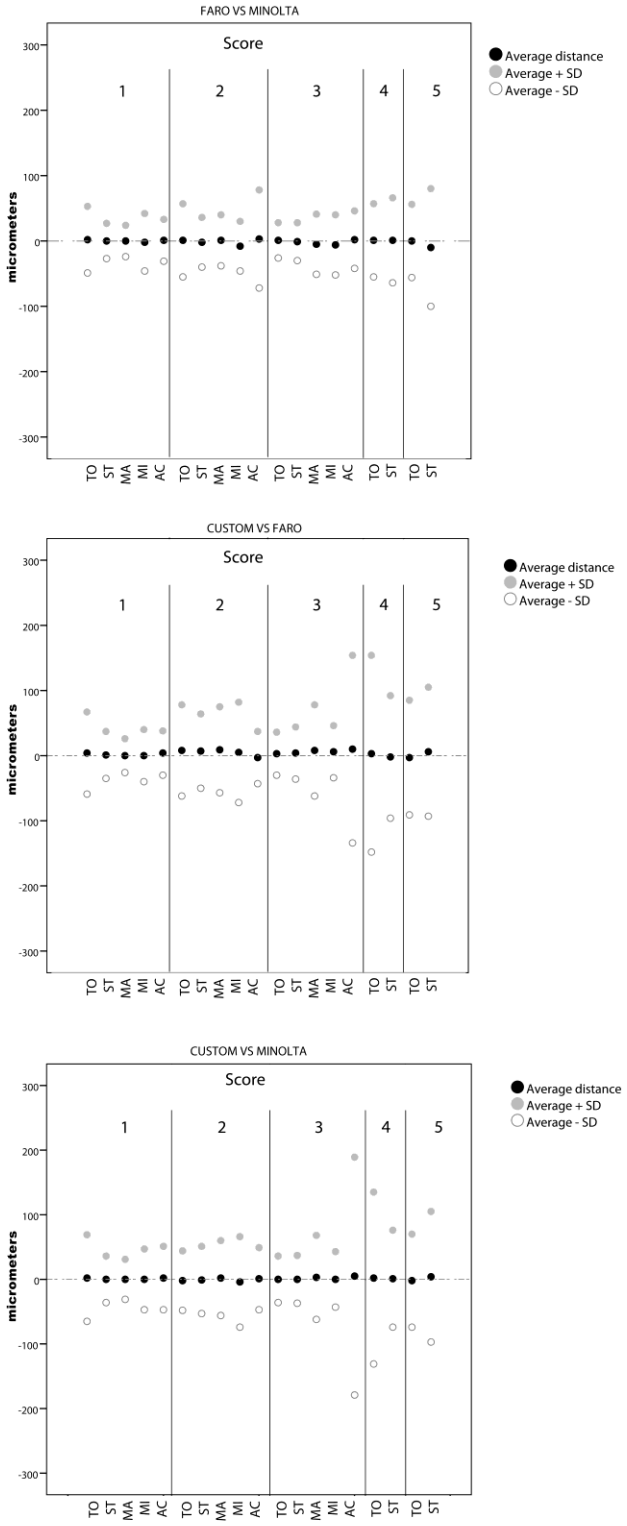

Villa C., Gaudio D., Cattaneo C., Buckberry J.,Wilson AS., Lynnerup N. 2015. *Surface curvature of pelvic joints from three laser scanners: separating anatomy from measurement error*. Journal of Forensic Sciences Vol. 60, No. 2, 2015, p. 374–381.

Figure 3: Pubic bone distance deviation; females (left) males (right)

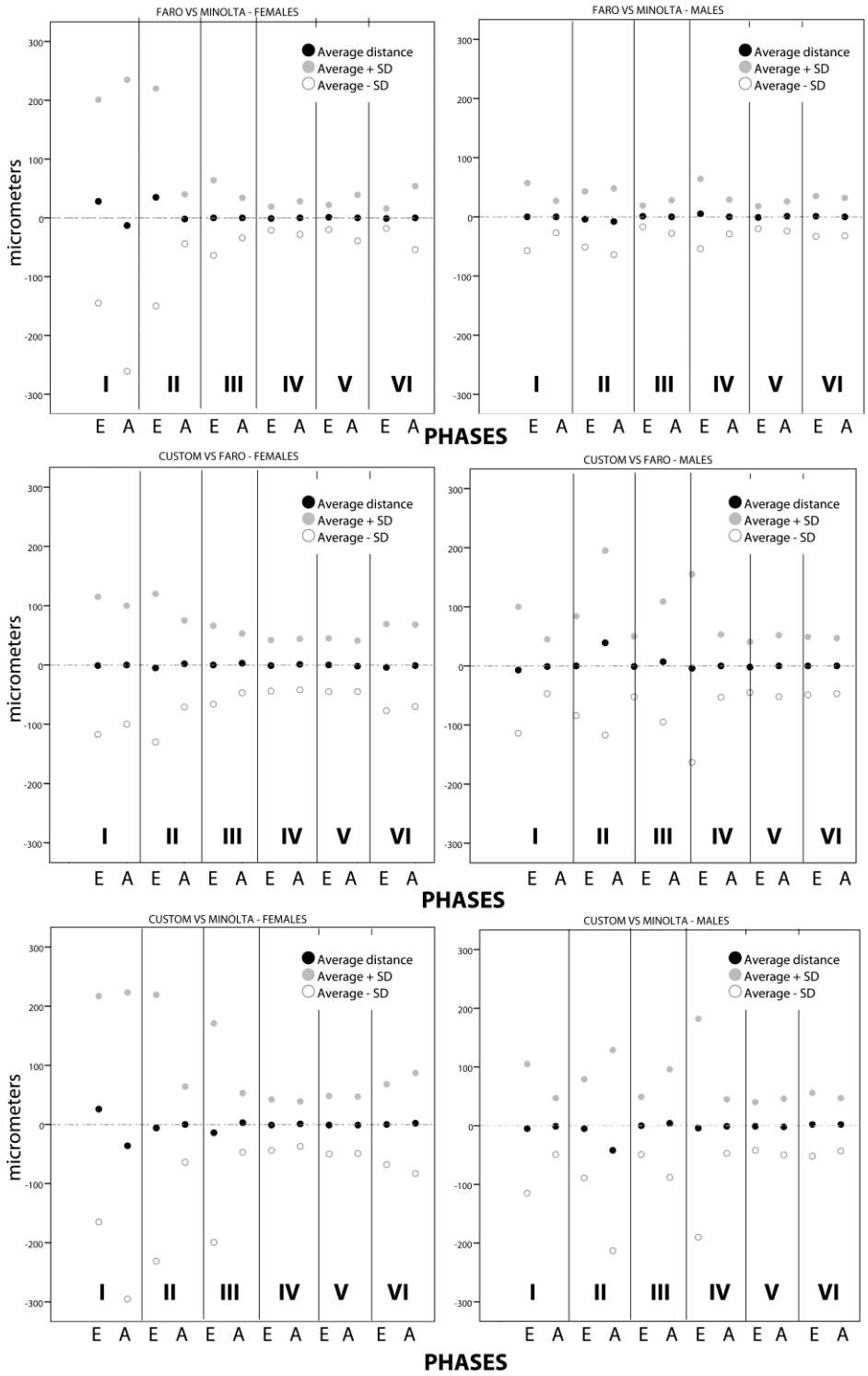

Figure 4: Color-coded mapping of the differences between laser scans for the female phase VI advanced pattern. The larger distances are marked by red and blue colors. Differences between 0.05 and -0.05 are indicated with green.